Chinese Journal of Physics 73 (2021) 275–287

Contents lists available at ScienceDirect

Chinese Journal of Physics

journal homepage: www.sciencedirect.com/journal/chinese-journal-of-physics

Dynamics of aluminum oxide and copper hybrid nanofluid in nonlinear mixed Marangoni convective flow with entropy generation: Applications to renewable energy

Yun-Xiang Li [a], M. Ijaz Khan [b], R. J. Punith Gowda [c], Arfan Ali [d], Shahid Farooq [b], Yu-Ming Chu [e,*], Sami Ullah Khan [f]

[a] School of Science, Hunan City University, Yiyang 413000, PR China
[b] Department of Mathematics and Statistics, Riphah International University I-14, Islamabad 44000, Pakistan
[c] Department of Studies and Research in Mathematics, Davangere University, Davangere, Karnataka, India
[d] Department of Management Science, Shaheed Zulfikar Ali Bhutto Institute of Science and Technology (SZABIST), Larkana Campus, Sindh, Pakistan
[e] Department of Mathematics, Huzhou University, Huzhou 313000, PR China
[f] Department of Mathematics, COMSATS University Islamabad, Sahiwal 57000, Pakistan

ARTICLE INFO

Keywords:
Marangoni convections
$Al_2O_3 - Cu - H_2O$;hybrid nanofluid flow
Non-linear heat source/sink
Viscous dissipation
Non-linear convection

ABSTRACT

One of the hottest topics in industrial and engineering applications of applied mathematics is the advances in nanotechnology particularly in nanofluids, hybrid nanofluids which consist of a typical base fluid saturated with nano-size metallic particles with enhanced thermophysical properties. In this regard, current study reports an entropy nature of steady, laminar, relative contributions of thermal and solutal Marangoni convections on passage in Casson $Al_2O_3 - Cu - H_2O$ hybrid nanofluid stream past over a disk under the impact of nonlinear heat source/sink, viscous dissipation, radiation, and nonlinear convection. Suitable similarity transformation is apt to reduce the governing partial differential equations to a series of ordinary differential equations. The obtained nonlinear ODE set is then solved numerically by using bvp4c method. The impact of various pertinent flow parameters on the velocity, thermal, concentration, entropy production, rate of heat and mass transfer fields are discussed in detail through graphs. The results reveal that, boost up values of Marangoni number and radiation parameter inclines the heat transfer of the fluid flow system. The upsurge in Exponential heat source/ sink parameter and thermal source/ sink parameter inclines the thermal profile. Further, increase in value of volume fraction inclines the rate of mass transfer.

1. Introduction

The investigation of non-Newtonian liquids has gotten a lot of attention because of the wide range of applications they have in industry and engineering, particularly in crude oil extraction from petroleum products. The recent development of several hypotheses has resulted from the consideration of non-Newtonian liquid in addition to classical Cauchy stress. Among such liquids, Casson fluid is a shear thinning liquid with unique characteristics. In 1995, Casson proposed this model for the viscoelastic liquids flow. Fuel engineers use this model to describe adhesive slurry. Recently, Sohail et al. [1] explained the features of entropy production in the stream of

* Corresponding author.
E-mail address: chuyuming@zjhu.edu.cn (Y.-M. Chu).

https://doi.org/10.1016/j.cjph.2021.06.004
Received 28 September 2020; Received in revised form 3 June 2021; Accepted 9 June 2021
Available online 16 June 2021

Nomenclature

(u,w)	Velocity components
g	Gravity
T	Temperature
μ	Dynamic viscosity
k	Thermal conductivity
k^*	Mean absorption co-efficient
Q_e	Exponential heat source coefficient
Ω	Constant
σ	Surface tension
D	Diffusion
γ_C	Rate of change of surface tension with respect to fluid concentration
R^*	Gas constant
β	Porosity parameter
β_t	Nonlinear thermal buoyancy parameter
ρ	Density
N^*	Ratio of thermal to solutal buoyancy forces
Pr	Prandtl number
A	Dimensionless parameter
Ec	Eckert number
$\gamma_1,\gamma_2,\gamma_3,\gamma_4$	Linear and nonlinear thermal and solutal
δ_1	Temperature difference parameter
δ_2	Solutal difference parameter
Br	Brinkman number
L	diffusion parameter
(r,z)	Directions
β	Casson parameter
ν	Kinematic viscosity
K^*	Porous medium permeability
σ^*	Boltzman constant
ρC_p	Specific heat capacitance
h	Exponential index
σ_0	Surface tension at the interface
Q_t	Heat sink/source parameter
γ_T	Rate of change of surface tension with respect to fluid temperature
B	Dimensionless parameter
β	Casson parameter
Sc	Schmidt number
λ	Mixed convection parameter
N_G	Entropy generation
β_c	Nonlinear solutal buoyancy parameter
R	Radiation parameter
Ma	Marangoni number

Subscript

f	Fluid
bf	Base fluid
hnf	Hybrid nanofluid
∞	Ambient
o	Surface

Casson liquid past an extending surface. Salahuddin et al. [2] elucidated the Casson liquid flow over an exponentially stretchy surface by considering the activation energy. Farooq et al. [3] explicated the Darcy-Forchheimerflow of Casson liquid over a permeable media. Lund et al. [4] inspected the aspect of dissipation effect on the radiative stream of Casson liquid past a surface. Kumar et al. [5] scrutinized the chemical reactiveCassonnanoliquid stream past a curved stretching surface.

Because of its global applications, the Marangoni convection phenomenon has piqued the interest of scholars and scientists. Marangoni convection is caused by changes in surface tension gradients, and it has applications in silicon wafer drying, crystal growth, soap film stabilization, and welding. Motivated by these applications, Qayyum [6] explicated the Marangoni convective stream of a

liquid suspended with more than on nanoparticles. Abdullah et al. [7] elucidated the Marangoni convective flow of a nanofluid by considering the thermophoresis and Brownian diffusion. Khan et al. [8] debriefed the heat generation in the Marangoni convective stream of a liquid over a disk with rotation. Jawad et al. [9] explicated the aspects of radiation on the Marangoni convective stream of nanoliquidabove an upright porous surface. Hayat et al. [10] elucidated the consequence of viscous dissipation on the viscoelastic liquid flow by considering the Marangoni convection.

In the fields of engineering and science, the most demanding applications of nanofluids are of great concern. The application of nanotechnology in contemporary science drew researchers to investigate nanofluid models from various perspectives. Nanofluids are made up of nanoparticles sized 1–100 nm suspended in a base fluid. Shape of the nanoparticles is fine spherical. Nanoparticles size is choose to be so small because for smaller particles there is a greater surface area as compared to the large sized particles of same mass. As we know that the ion release from the surface area, the greater the surface area there is greater release of ions. And this is the only reason why nanoparticles are taken to be so small in size because they have more antibacterial effect as they release more ions than the larger particles per unit mass. A hybrid nanofluid is made up of two separate -nanosized particles combined with a base fluid. Other than the atypically high effective thermal conductivity, hybrid nanofluid can provide great benefits when the nanosized particles are adequately dispersed. Hybrid nanofluid has been introduced to investigate the properties of heat transfer and make it even better. Heat transference in the fields of microelectronics, microfluidics, manufacturing and medical are few of the applications for hybrid nanofluids. Jayadevamurthy et al. [11] elucidated the bioconvective flow of a hybrid nanoliquid past a poignant disk. Khan et al. [12] inspected the ohmic heating effect on the stream of hybrid nanoliquid between two parallel plates. Christopher et al. [13] discussed the flow of a liquid withdual nanoparticles suspension through a permeable medium. Abbas et al. [14] debriefed magnetically triggered flow of hybridnanoliquid through a cylinder. Kumar et al. [15] delineated the hybrid nanoliquid flow with the impact of magnetic dipole through an extending cylinder.

Heat transfer plays a prominent role in many noteworthy applications in several industrial and engineering processes. The effective addition of heat, transforming heat from one place to another, and regulating the heat will stable the heat transfer process. The transfer of heat takes place due to various causes like non-linear heat source/sink, viscous dissipation and so on. So, the energy equation has been formulated by including all the necessary associated terms which explain the heat transfer features. Recently, Irfan et al. [16] examined the consequence of non-linear heat generation /absorption on the nanoliquid flow. Ramzan et al. [17] inspected the major influence of non-uniform heat sink/source on the liquid flow over a thin needle with motion. Radhika et al. [18] explained the non-linear heat sink/source effects on the dusty hybrid nanoliquidflowabove a surface. Ali et al. [19] probed the heat source/absorption impact on the stream of third-grade liquid above a stretchy cylinder. Faisal et al. [20] discussed the non-linear heat generation/sink effects on the flow of nanoliquid past an expandable surface. Xiong et al. [21] explicated the significant aspects of viscous dissipation on the cross nanofluid flow through a needle placed in a porous media. Lund et al. [22] inspected the dissipative two-dimensional stream of a liquid suspended with dual nanoparticles suspension over a permeable surface. Shah et al. [23] elucidated the flow of nanoliquid between the permeable plates by considering the viscous dissipation. Hong et al. [24] inspected the nonlinear convective heat transference in the stream through a permeable cylinder. Idowu et al. [25] discussed the nonlinear convective stream of Cassonnanoliquid through a permeable channel. Rashad et al. [26] addressed the thermally stratified flow of nanofluid over vertical cylinder. El-Kabeir et al. [27] discussed the radiative analysis for the nanofluid flow in a porous space. Mansour et al. [28] examined the heat transfer enhancement in hybrid nanoparticles flow with entropy generation features. EL-Zahar et al. [29] inspected the mixed convection flow of radiative nanoparticles in presence of magnetic force. Tehrani et al. [30] analyzed the dispersion of nanoparticles over vertical duct numerically. The optimized features of copper and water based nanofluids in square duct were examined by Vasefi et al. [31]. In another useful contribution, Vasefi et al. [32] presented the impressive enhancement in heat transfer by using CuO/-Water in horizontal channel. Tehrani et al. [33] addressed the applications of nanoparticles in ribbed flat-plate solarcollector. The work of Tehrani et al. [34] presented the thermal transport nanofluids in a vertical duct. The forced convection of nanofluids with turbulent flow behavair was examined by Tehrani et al. [35]. Lin and Zheng [36] analyzed the improvement in heat transfer by utilizing the copper-water nanofluid.

According to the available literature, thermal and solutal Marangoni convections on transport in Casson hybrid nanofluid flow past over a rotating disk are extremely rare, and none of the published articles separately the effect of nonlinear heat source/sink, viscous dissipation, radiation, and nonlinear convection on such fluid stream. Hence to bridge the gap, we discussed the thermal and solutal Marangoni convections on transport in Casson hybrid nanofluid flow past over a rotating disk under the impact of nonlinear heat source/sink, viscous dissipation, radiation, and nonlinear convection.

2. Mathematical formulation

The laminar, steady, incompressible, and two-dimensional thermal and solutal Marangoni convective flow of dissipating Casson $Al_2O_3 - Cu - H_2O$hybrid nanofluid over a disk is considered taking account of nonlinear heat source/sink, and nonlinear convection. Flow is caused due to temperature and concentration gradients created surface tension.Temperature and concentration vary at the surface.

The governing (continuity, momentum and energy) equations under incompressible, constant properties and steady-state conditions take the form [6], [7, 8] and [9]

$$\frac{\partial u}{\partial r} + \frac{u}{r} + \frac{\partial w}{\partial z} = 0, \tag{1}$$

$$u\frac{\partial u}{\partial r}+w\frac{\partial u}{\partial z}=\nu_{hnf}\left(1+\frac{1}{\beta_1}\right)\frac{\partial^2 u}{\partial z^2}-\frac{\nu_{hnf}}{K^*}u+g\left[\begin{matrix}(T-T_\infty)\lambda_1+\lambda_2(T-T_\infty)^2+\\ \lambda_3(C-C_\infty)+\lambda_4(C-C_\infty)^2\end{matrix}\right], \tag{2}$$

$$\left.\begin{matrix}u\frac{\partial T}{\partial r}+w\frac{\partial T}{\partial z}=\frac{k_{hnf}}{(\rho C_p)_{hnf}}\frac{\partial^2 T}{\partial z^2}+\frac{16\sigma^* T_\infty^3}{(\rho C_p)_{hnf}3k^*}\frac{\partial^2 T}{\partial z^2}+\\ \frac{Q_e(T_0-T_\infty)}{(\rho C_p)_{hnf}}\exp\left[-h\sqrt{\nu_f\Omega}\,z\right]+\frac{Q_l(T-T_\infty)}{(\rho C_p)_{hnf}}+\frac{\mu_{hnf}}{(\rho C_p)_{hnf}}\left(1+\frac{1}{\beta_1}\right)\left(\frac{\partial u}{\partial z}\right)^2\end{matrix}\right\}, \tag{3}$$

$$u\frac{\partial C}{\partial r}+w\frac{\partial C}{\partial z}=D\frac{\partial^2 C}{\partial z^2}. \tag{4}$$

Here boundary conditions are studied at $z\to 0$and$z\to\infty$. First equation in B.C's is due to Marangoni convection of Casson fluid. $w=0$shows that velocity in w direction is zer0 at $z=0$, temperature and concentration at disk are shown to be T_0 *and* C_0 in 3rd and 4th equation. Also we can see that far away from the disk motion of the fluid approaches to zero also temperature and concentration of the fluid are T_∞ and C_∞.

$$\left.\begin{matrix}z=0:\mu_{hnf}\left(1+\frac{1}{\beta_1}\right)\frac{\partial u}{\partial z}=-\frac{\partial\sigma}{\partial r}=\sigma_0\left(\gamma_T\frac{\partial T}{\partial x}+\gamma_C\frac{\partial C}{\partial x}\right), w=0, T=T_0=T_\infty+Ar^2, C=C_0=C_\infty+Br^2,\\ z\to\infty: u\to 0, T\to T_\infty, C\to C_\infty.\end{matrix}\right\}. \tag{5}$$

The surface tension $\sigma=\sigma_0[1-\gamma_T(T-T_\infty)-\gamma_C(C-C_\infty)]$ is supposed to depend on linear fluctuation with temperature and concentration boundaries. Where the surface tension coefficients for temperature is $\gamma_T=-\frac{1}{\sigma_0}\frac{\partial\sigma}{\partial T}|_{T=T_\infty}$ and concentration is $\gamma_C=-\frac{1}{\sigma_0}\frac{\partial\sigma}{\partial C}|_{C=C_\infty}$.

Following similarity transformation procedure is employed:

$$\left.\begin{matrix}u=r\Omega f, w=\sqrt{\Omega\nu_f}h, \xi=z\sqrt{\frac{\Omega}{\nu_f}},\\ T=T_\infty+Ar^2\theta, C=C_\infty+Br^2\varphi,\end{matrix}\right\}. \tag{6}$$

Entropy generation

$$\left.\begin{matrix}S_G=\frac{1}{T_\infty^2}\left\{\frac{k_{hnf}}{(\rho C_p)_{hnf}}+\frac{16\sigma^* T_\infty^3}{(\rho C_p)_{hnf}3k^*}\right\}\frac{\partial^2 T}{\partial z^2}+\\ \frac{\mu_{hnf}}{T_\infty}\left(1+\frac{1}{\beta_1}\right)\left(\frac{\partial u}{\partial z}\right)^2+\frac{\mu_{hnf}}{K^*T_\infty}u^2+\frac{R^*D}{T_\infty}\frac{\partial T}{\partial z}\frac{\partial C}{\partial z}+\frac{R^*D}{C_\infty}\left(\frac{\partial C}{\partial z}\right)^2\end{matrix}\right\}. \tag{7}$$

The reduced non-dimensional form of assumed mathematical model is as follow:

$$h'+2f=0, \tag{8}$$

$$\frac{1}{A_1A_2}\left(1+\frac{1}{\beta_1}\right)f''-hf'+f^2-\frac{\beta}{A_1A_2}f+\frac{1}{A_2}\lambda\theta(1+\beta_t\theta)+\lambda\varphi N^*(1+\beta_c\varphi)=0, \tag{9}$$

$$\frac{1}{\mathrm{Pr}}\left(\frac{k_{hnf}}{k_f}+R\right)\theta''-(2f\theta+h\theta')+\frac{Q}{A_4}\theta\exp(-n\xi)+\frac{Q_t}{A_4}\theta+\frac{1}{A_1A_4}\left(1+\frac{1}{\beta_1}\right)Ecf'^2=0, \tag{10}$$

$$\frac{1}{Sc}\varphi''-(2f\varphi+H\varphi')=0. \tag{11}$$

The transformed boundary conditions are:

$$\left.\begin{matrix}\left(1+\frac{1}{\beta}\right)\frac{1}{A_1}f'(0)=-2Ma(1+R), h(0)=0, \theta(0)=1, \varphi(0)=1,\\ f(\infty)\to 0, \theta(\infty)\to 0, \varphi(\infty)\to 0.\end{matrix}\right\}. \tag{12}$$

2.1. Analysis of entropy

Entropy generation is the amount of entropy during any irreversible process. Heat and mass transfer processes including fluid flow, mixing of substances, expansion of matters, heat exchange and motion of bodies. Entropy generation minimization is important for increasing the performance of the system. When there is less irreversibility in the system very less energy loss occurs. Entropy generation rate in presence of heat transfer irreversibility, mass transfer irreversibility, porous medium irreversibility, thermal radiation irreversibility and viscous dissipation irreversibility in its dimensionless form is given by:

$$N_G = \left(\frac{k_{hnf}}{k_f} + R\right)\delta_1\theta'^2 + \frac{\beta Br}{(1-\varphi_1)^{2.5}(1-\varphi_2)^{2.5}}f^2 + Br\left(1+\frac{1}{\beta_1}\right)f''^2 + L\theta'\varphi' + L\frac{\delta_2}{\delta_1}\varphi'^2, \tag{13}$$

where

$$A = (T_0 - T_\infty), B = (C_0 - C_\infty), \Pr = \frac{\mu_f}{\alpha_f}, \beta = \frac{\nu_f}{K^*\Omega}, = \frac{16\sigma^* T_\infty^3}{3k^* k_f}, \lambda = \frac{g(\gamma)_1(T_0 - T_\infty)}{r\Omega^2}, Sc = \frac{\nu_f}{D_B},$$

$$\beta_t = \frac{\gamma_2}{\gamma_1}(T_0 - T_\infty), \beta_c = \frac{\gamma_4}{\gamma_3}(C_0 - C_\infty), N^* = \frac{\gamma_3}{\gamma_1}\frac{(C_0 - C_\infty)}{(T_0 - T_\infty)}, Q = \frac{Q_e}{(\rho C_p)_f\Omega}, Q_t = \frac{Q_l}{(\rho C_p)_f\Omega}, \tag{14}$$

$$Ec = \frac{r^2\Omega^2}{C_p(T_0 - T_\infty)}, Ma = \frac{\gamma_T A}{\mu_f\Omega}\sqrt{\frac{\nu_f}{\Omega}}, \gamma = \frac{\gamma_C B}{\gamma_T A}, \delta_1 = \frac{T_0}{T_\infty}, \delta_2 = \frac{C_0}{C_\infty}, N_G = \frac{S_G T_\infty \nu_f}{k_f \Delta T \Omega}, Br = \frac{r^2\Omega^2\mu_f}{k_f\Delta T\Omega}, L = \frac{R^* DBr^2}{k_f},$$

Table 1 and Table 2 are constructed for mathematical expressions and numerical values of thermophysical properties. The engineering physical interest quantity, Nusselt number and local Sherwood number are as follow:

$$Nu_x = \frac{r\left[-\frac{\partial T}{\partial r}\Big|_{z=0} + q_r|_{z=0}\right]}{k_f(T_0 - T_\infty)}, Sh_x = -\frac{r\frac{\partial C}{\partial z}}{D(C_0 - C_\infty)}$$

Non-dimensional Nusselt number and local Sherwood number are given by:

$$\frac{Nu_x}{\sqrt{\mathrm{Re}_x}} = -\left(\frac{k_{hnf}}{k_f} + R\right)\theta'(0), \frac{Sh_x}{\sqrt{\mathrm{Re}_x}} = -\varphi'(0).$$

3. Validation

Table 3 presents the comparison of obtained numerical results with work of Lin and Zheng [36] as a limiting case. A good agreement between both investigations is noted.

4. Result and discussion

An entropy nature of a steady Marangoni Casson hybrid nanofluid flow past over a disk is securitized by considering nonlinear heat source/sink, viscous dissipation and nonlinear convection.The nonlinear boundary value problem comprised in the model are tackled using bvp4c MATLAB method. This method is used to solve the ordinary differential boundary value problem. Each method has some advantages and disadvantages so as bvp4c MATLAB have. The main advantage is that it accept multipoint BVP's directly whereas many other solvers do not. Source of the code is available so we can easily modify the code for existing equations at no cost. MATLAB is interpreted language so it is easy to fix the errors. There are also some disadvantages of it that it only solves first order differential equation. Higher orders cannot be solved in bvp4c MATLAB method firstly you have to convert your system in to first order. As it is mentioned earlier that MATLAB is interpreted language so it takes more time to execute as compared to C and C++. The main aim of this section is to frame and elaborately reconnoiter the characters of dimensionless parametric influence on the flow, concentration, temperature, Nusselt and Sherwood numbers. To clearly check the insight of proposed model, we have chosen a variety range of values of parameters to simulate the process. The convergence of these series strongly depends upon the value of these parameters. The effects are revealed and displayed graphically Figs. (1–20).

Figs. 1–7 display fluctuation in velocity gradient for varied values of non-dimensional physical parameters. Fig. 1 is designed to illustrate the influence of β on velocity profile. Here, increase in value of βdeclines the velocity profile. This is due to the resistive power

Table 1
Mathematical expressions for thermophysical properties of hybrid nanofluid.

Properties	$Al_2O_3 - \mathbf{Cu} - \mathbf{H_2}O$
Density(ρ)	$A_2 = \frac{\rho_{\mathrm{hnf}}}{\rho_{\mathrm{f}}} = (1-\varphi_2)\left[(1-\varphi_1) + \varphi_1\frac{\rho_{s1}}{\rho_{\mathrm{f}}}\right] + \varphi_2\frac{\rho_{s2}}{\rho_{\mathrm{f}}}$
Heat capacity (ρC_p)	$A_4 = \frac{(\rho \mathrm{Cp})_{\mathrm{hnf}}}{(\mathrm{C_p}\rho)_{\mathrm{f}}} = (1-\varphi_2)\left[(1-\varphi_1) + \varphi_1\left(\frac{(\rho\mathrm{Cp})_{s1}}{(\rho\mathrm{Cp})_{\mathrm{f}}}\right)\right] + \varphi_2\frac{(\rho\mathrm{Cp})_{s2}}{(\rho\mathrm{Cp})_{\mathrm{f}}},$
Viscosity (μ)	$A_1 = \mu_{\mathrm{hnf}}/\mu_{\mathrm{f}} = (1-\varphi_1)^{2.5}(1-\varphi_2)^{2.5}$
Thermal conductivity	$\frac{\mathrm{k_{hnf}}}{\mathrm{k_{bf}}} = \frac{\mathrm{k_{s_2}} + 2\mathrm{k_{bf}} - 2\varphi_2(\mathrm{k_{bf}} - \mathrm{k_{s_2}})}{\mathrm{k_{s_2}} + 2\mathrm{k_{bf}} + \varphi_2(\mathrm{k_{bf}} - \mathrm{k_{s_2}})},$ $\frac{\mathrm{k_{bf}}}{\mathrm{k_f}} = \frac{\mathrm{k_{s_1}} + 2\mathrm{k_f} - 2\varphi_1(\mathrm{k_f} - \mathrm{k_{s_1}})}{\mathrm{k_{s_1}} + 2\mathrm{k_f} + \varphi_1(\mathrm{k_f} - \mathrm{k_{s_1}})},$ $A_4 = \frac{\mathrm{k_{hnf}}}{\mathrm{k_f}}$
Prandtl number	6.2

Table 2
Thermophysical properties of density, thermal conductivity, specific heat and thermal expansion.

Physical properties	ρ (kg /m^3)	C_p (J /kgK)	k (W /mK)	Pr
Al_2O_3	3970	765	40	–
Cu	8933	385	401	—-
H_2O	997.1	4179	0.613	6.2

Table 3
Comparative result of $f(0)$ and $H(\infty)$ with Lin and Zheng [36] when $\varphi_1 = \beta = \beta_1 = \lambda = R = 0$ and $Ma = 0.2$.

Parameter	Lin and Zheng [36]				Present results	
	$f(0)$			$h(\infty)$	$f(0)$	$h(\infty)$
φ_2	HAM	Numerical	HAM	Numerical	Bvp4c	Bvp4c
0.0%	0.307593	0.3073370	-0.835982	-0.831657	0.3073359	-0.831649
1.5%	0.292523	0.2922949	−-0.785369	-0.781320	0.2922913	-0.781318
3.0%	0.279196	0.2789964	−-0.743459	-0.739749	0.2789954	-0.739739
4.5%	0.267258	0.2670791	-0.708301	-0.704876	0.2670787	-0.704870

generated by the permeable region. The liquid has more space to flow when the porousness is massive, i.e., when it is decreasing. As a result, the velocity increases. Fig. 2 describes how β_1 engulfs the velocity profile both in radial and vertical directions. Result reveals that the rise in β_1 increases the velocity gradient in both the directions. Consequence of velocity profile for various values $\lambda$is displayed in Fig. 3. Rise in values of λincrease the velocity profile. As a result, the buoyancy parameter's velocity profile and momentum boundary layer thickness are improved. The ratio of buoyancy to inertial forces is demarcated as mixed convection. For biggerλ, buoyancy force dominates inertial force, which increases fluid velocity. Figs. 4 and 5 are depicted to show the domination of volume fraction over a velocity profile in both radial and vertical direction. Upsurge in φ_1 and $\varphi_2$declines velocity and momentum of the fluid flow in both directions. In fact, compared to dense materials, energy transport in metallic-type materials is faster. Due to the reason velocity profile decreases for increase in volume fractions $\varphi_1$andφ_2. Figs. 6 and 7 establishes the flow pattern of velocity gradient in both radial and vertical direction for increasing values of *Ma*and *r* respectively. Higher the values of both *Ma* and *r*improves the velocity of the flow in both the direction as show in the figure.

Figs. 8–12 demonstrate the Change in thermal gradient for varied values of different dimensionless parameters. Fig. 8 describes the variation of thermal profile in response to varied values of *Ma*. The figure explores that the shoot-up values of *Ma* upsurges the thermal profile gradually. The surface tension caused by thermosolutal gradients is the reason for this upsurge. Fig. 9 shows the behavior of heat transference for increasing values ofβ_1. Here, incline in β_1 inclines the thermal profile. Figs. 10 and 11 are portrayed to explain the impact of Q and Q_t subjected to temperature profile. Here, increase in values of both the parameter Q and Q_t inclines the thermal profile. Moreover, as the Q and Q_t increases, the strength of the heat source process increases, resulting in more heat being transferred to the liquid and therefore an increase in θ(ξ). Fig. 12 demonstrates the influence of radiation parameter R on thermal profile. Emission of electromagnetic waves from all sources is called thermal radiation that has temperature greater than zero. Due to thermal radiation electromagnetic energy formed by conversion of thermal energy where thermal energy is also known as kinetic energy of irregular movement of atoms and molecules in matter. It is apparent from the sketch that upsurge in radiation parameter enhances the heat transference. The strengthening of parameter R transferences more heat into the fluid and increases the thickness of the thermal boundary layer. Physically it is due to the fact that for higher radiation parameter mean absorption coefficient decays hence temperature enhances.

Figs. 13–14 illustrate the performance of Concentration profile for numerous varied parameters. Fig. 13 plots the aspects of *Sc* on concentration profile. The growth in values of *Sc* declines the mass transfer. Mathematically, a dimensionless number relating mass diffusivity with momentum diffusivity yielding a fluid flow is treated as Schmidt number. These two terms are physically called the

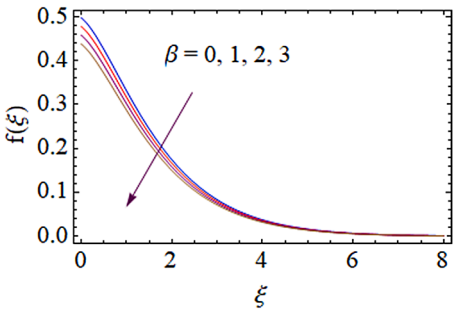

Fig. 1. Encouragement of β on $f(\xi)$.

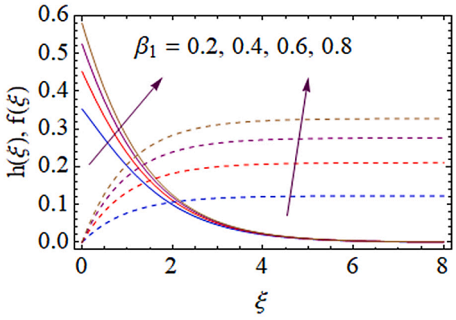

Fig. 2. Encouragement of β_1 on $h(\xi)$,$f(\xi)$.

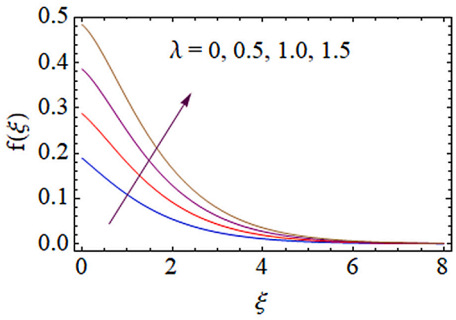

Fig. 3. Encouragement of λ on $f(\xi)$.

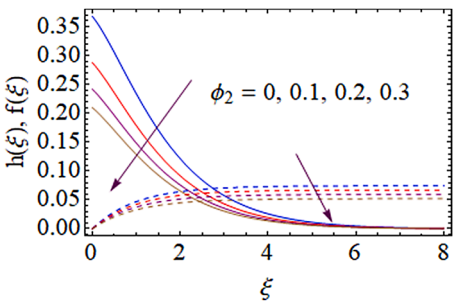

Fig. 4. Encouragement of φ_2 on $h(\xi)$,$f(\xi)$.

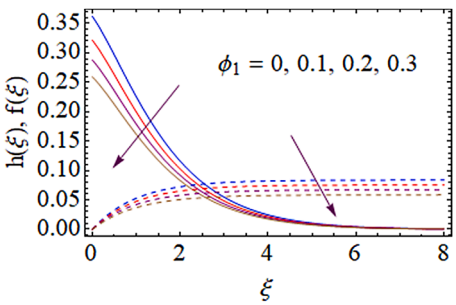

Fig. 5. Encouragement of φ_1 on $h(\xi)$,$f(\xi)$.

hydrodynamic thickness layer and mass transport layer. The declination in concentration field due to mass diffusion occurs for an enhancement in the Sc. The encouragement of *Ma* over mass distribution is portrayed in Fig. 14. Figure clearly shows that, the growing values of *Ma* declines the concentration gradient.

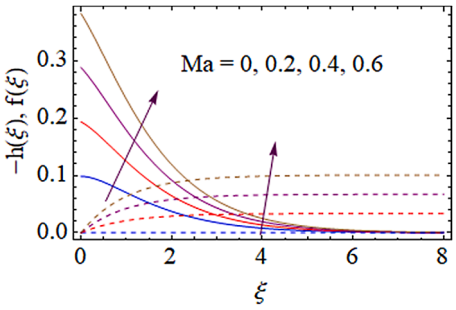

Fig. 6. Encouragement of *Ma* on $-h(\xi), f(\xi)$.

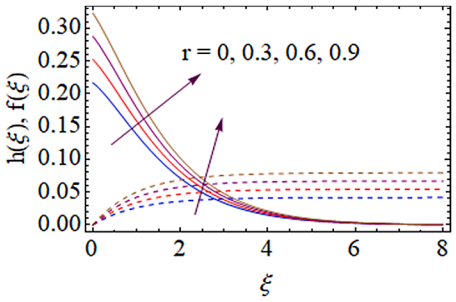

Fig. 7. Encouragement of r on $h(\xi), f(\xi)$.

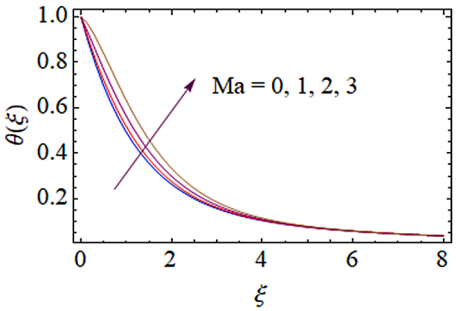

Fig. 8. Encouragement of *Ma* on $\theta(\xi)$.

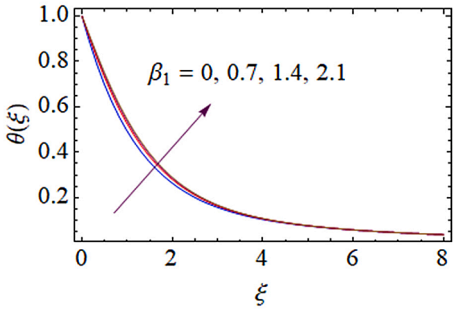

Fig. 9. Encouragement of β_1 on $\theta(\xi)$.

Figs. 15–18 enclose the behavior of entropy generation profile for various parameters. The influence of *Ma*on entropy generation rate is shown in Fig. 15. The upsurge in *Ma*improves the N_G. Further, N_G acts as growing function of *Ma*. The influence of *Br* on $N_G$is depicted in Fig. 16. Here, upsurge in *Br* declines the N_G. Physically, *Br* is accountable for the heat transference via dual chief sources, i.

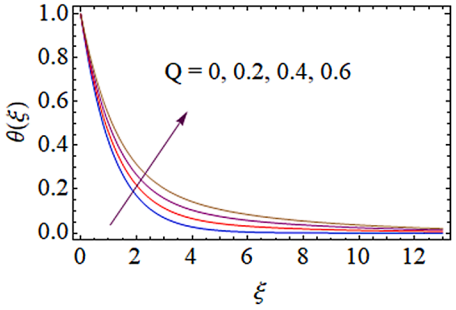

Fig. 10. Encouragement of Q on $\theta(\xi)$.

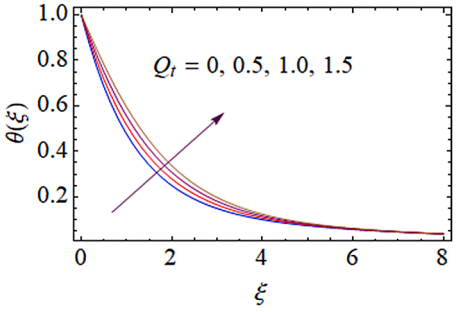

Fig. 11. Encouragement of Q_t on $\theta(\xi)$.

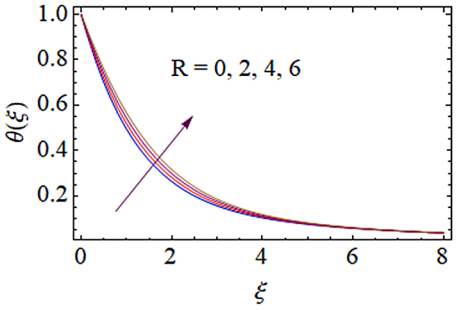

Fig. 12. Encouragement of R on $\theta(\xi)$.

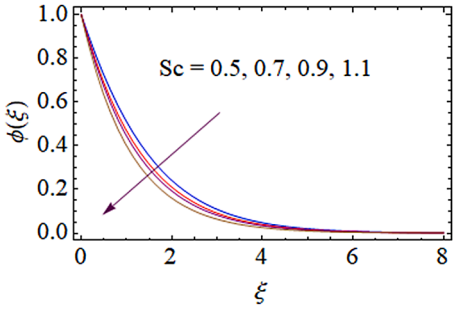

Fig. 13. Encouragement of Sc on $\varphi(\xi)$.

e., heat generated by viscous dissipation among heat conveyed by conduction and concurring layers of a nanomaterial.The sway of L on N_G is showed in Fig. 17. It is spotted from plotted graph that, boost up values of L improves the N_G. Moreover, N_G acts as growing function of L. The levering of $\varphi_2$on entropy generation profile is depicted in Fig. 18. Here, inclination in φ_2 improves the entropy

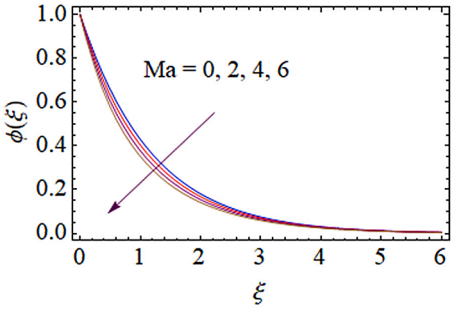

Fig. 14. Encouragement of *Ma* on $\varphi(\xi)$.

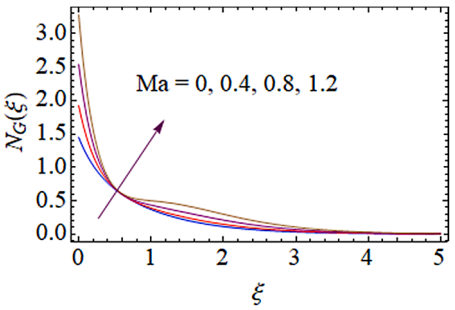

Fig. 15. Encouragement of *Ma* on $N_G(\xi)$.

generation rate. $N_G$acts as growing function of φ_2.

Graphical illustration of Nusselt and Sherwood numbers for several non-dimensional parameters are displayed in Figs. 19–20. The variation in Nusselt number against *R* for different values of *Ma*is portrayed in Fig. 19. One can notice from figure that, increase in *Ma*deteriorates the rate of heat transference and but converse trend can be observed for upsurge in values of *R*. Here, Nusselt number acts as a growing function of *R* and diminishing function of *Ma*. Fig. 20 imparts the actions of rate of mass transfer counter to *Sc*for diverse values of φ_1. Here φ_1 acts as inclining functions of rate Sherwood number.

5. Final remarks

In present study, we delineate the effects of steady, laminar, relative contributions of thermal and solutal Marangoni convections on transport in Casson hybrid nanofluid flow past over a disk by considering the nonlinear heat source/sink, viscous dissipation, radiation, and nonlinear convection. A special type of hybrid nanoliquid containing nanoparticles is considered in the model. By using similarity renovation foremost governing equations are reduced from PDE's to ODE's and later, these equations are solved numerically using bvp4c method. Influences of pertinent parameters on the flow, concentration, thermal and entropy generation are highlighted with the help of graphs. The concluded main findings are as follows:

- The upsurge of $\beta_1$values inclines fluid velocity and boundary layer thickness related to it in both radial and vertical directions.
- The fluid velocity decreases gradually in both radial and vertical directions with an augmentation of $\varphi_1$and φ_2.

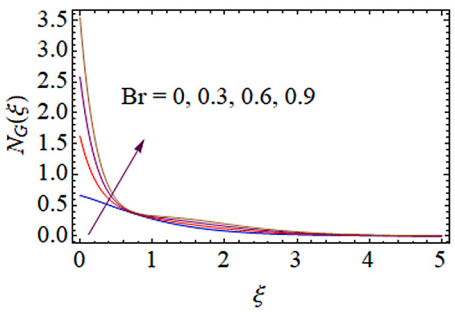

Fig. 16. Encouragement of *Br* on $N_G(\xi)$.

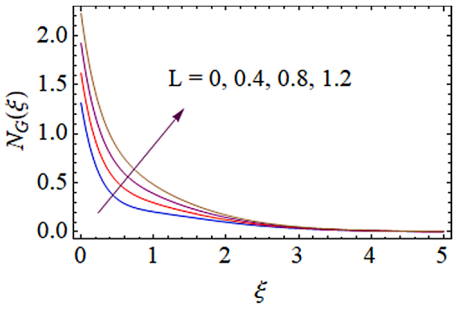

Fig. 17. Encouragement of L on $N_G(\xi)$.

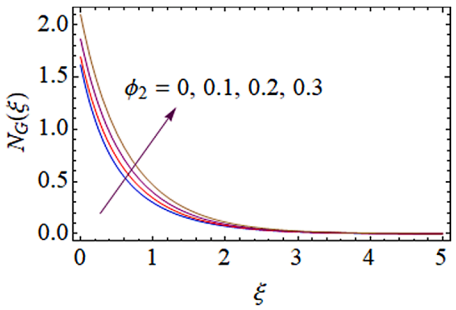

Fig. 18. Encouragement of φ_2 on $N_G(\xi)$.

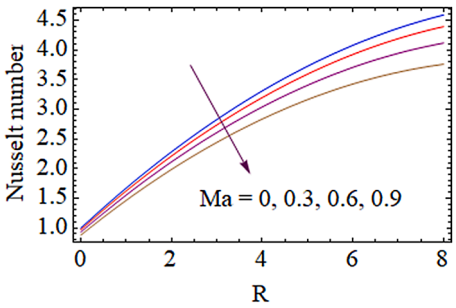

Fig. 19. Encouragement of *Ma* on*Nu*versus *R*.

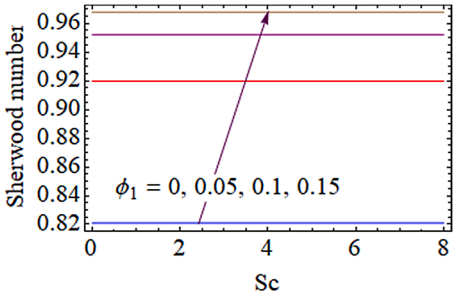

Fig. 20. Encouragement of φ_1 on*Sh*versus *Sc*.

- $\theta(\xi)$increases rapidly with upsurge in the values of *Ma*and *R*.
- The escalating values of *Q*and $Q_t$improves the thermal gradient.
- An an increment in the *Ma* and*R*values improve entropy production.
- The entropy production increases with an augmentation in the *Br* and as well as $\varphi_1$values.

v The Nusselt number exhibits increasing trend for enhancement of R, and acts as a declining function for Ma.
v The rate of mass transfer increases for enhancement of φ_1.

Declaration of Competing Interest

The authors declare that they have no known competing financial interests or personal relationships that could have appeared to influence the work reported in this paper.

Acknowledgments

Projects supported by the Natural Science Foundation of Hunan Province, China (Grant No.2018JJ2016), and the Key Laboratory of Key Technologies of Digital Urban-Rural Spatial Planning of Hunan Province (Grant No.2018TP1042).

References

[1] M. Sohail, Z. Shah, A. Tassaddiq, P. Kumam, P. Roy, Entropy generation in MHD Casson fluid flow with variable heat conductance and thermal conductivity over non-linear bi-directional stretching surface, Sci. Rep. 10 (1) (2020), https://doi.org/10.1038/s41598-020-69411-2.
[2] T. Salahuddin, M. Arshad, N. Siddique, A.S. Alqahtani, M.Y. Malik, Thermophyical properties and internal energy change in Casson fluid flow along with activation energy, Ain Shams Eng. J. 11 (4) (2020) 1355–1365, https://doi.org/10.1016/j.asej.2020.02.011.
[3] U. Farooq, M.A. Ijaz, M.I. Khan, S.S.P.M. Isa, D.C. Lu, Modeling and non-similar analysis for Darcy-Forchheimer-Brinkman model of Casson fluid in a porous media, Int. Commun. Heat Mass Transf. 119 (2020), 104955, https://doi.org/10.1016/j.icheatmasstransfer.2020.104955.
[4] L.A. Lund, Z. Omar, I. Khan, D. Baleanu, K.S. Nisar, Dual similarity solutions of MHD stagnation point flow of Casson fluid with effect of thermal radiation and viscous dissipation: stability analysis, Sci. Rep. 10 (1) (2020), https://doi.org/10.1038/s41598-020-72266-2.
[5] R.S.V. Kumar, P.G. Dhananjaya, R. Naveen Kumar, R.J.P. Gowda, B.C. Prasannakumara, Modeling and theoretical investigation on Casson nanofluid flow over a curved stretching surface with the influence of magnetic field and chemical reaction, Int. J. Comput. Methods Eng. Sci. Mech. 0 (2021) 1–8, https://doi.org/10.1080/15502287.2021.1900451.
[6] S. Qayyum, Dynamics of Marangoni convection in hybrid nanofluid flow submerged in ethylene glycol and water base fluids, Int. Commun. Heat Mass Transf. 119 (2020), 104962, https://doi.org/10.1016/j.icheatmasstransfer.2020.104962.
[7] A.A. Abdullah, N.M. Alraiqib, K.A. Lindsay, Modelling the stability of Marangoni convection in a layer of nanofluid, Int. J. Therm. Sci. 151 (2020), 106228, https://doi.org/10.1016/j.ijthermalsci.2019.106228.
[8] M.I. Khan, S. Qayyum, Y.-.M. Chu, N.B. Khan, S. Kadry, Transportation of Marangoni convection and irregular heat source in entropy optimized dissipative flow, Int. Commun. Heat Mass Transf. 120 (2021), 105031, https://doi.org/10.1016/j.icheatmasstransfer.2020.105031.
[9] M. Jawad, A. Saeed, P. Kumam, Z. Shah, A. Khan, Analysis of boundary layer MHD Darcy-Forchheimer radiative nanofluid flow with soret and dufour effects by means of marangoni convection," Case Stud, Therm. Eng. 23 (2021), 100792, https://doi.org/10.1016/j.csite.2020.100792.
[10] T. Hayat, S.A. Khan, A. Alsaedi, H.M. Fardoun, Marangoni forced convective flow of second grade fluid with irreversibility analysis and chemical reaction, Int. J. Thermophys. 42 (1) (2020) 11, https://doi.org/10.1007/s10765-020-02764-y.
[11] Punith Gowda RamanahalliJayadevamurthy, Naveen kumar Rangaswamy, B.C Prasannakumara, K.S Nisar, Emphasis on unsteady dynamics of bioconvective hybrid nanofluid flow over an upward–downward moving rotating disk, Numer. Methods Partial Differ. Equ. (2020), https://doi.org/10.1002/num.22680.
[12] M. Ijaz Khan, M.U. Hafeez, T. Hayat, M. Imran Khan, A. Alsaedi, Magneto rotating flow of hybrid nanofluid with entropy generation, Comput. Methods Programs Biomed. 183 (2020), 105093, https://doi.org/10.1016/j.cmpb.2019.105093 doi.
[13] A.J. Christopher, N. Magesh, R.J. Punith Gowda, R. Naveen Kumar, R.S.V. Kumar, Hybrid nanofluid flow over a stretched cylinder with the impact of homogeneous–heterogeneous reactions and Cattaneo–Christov heat flux: series solution and numerical simulation, Heat Transf (2020), https://doi.org/10.1002/htj.22052.
[14] N. Abbas, S. Nadeem, A. Saleem, M.Y. Malik, A. Issakhov, F.M. Alharbi, Models base study of inclined MHD of hybrid nanofluid flow over nonlinear stretching cylinder," Chin, J. Phys. 69 (2021) 109–117, https://doi.org/10.1016/j.cjph.2020.11.019.
[15] R Naveen Kumar, R.J. Punith Gowda, Abdullah M Abusorrah, Y.M. Mahrous, Nidal H Abu-Hamdeh, AlibekIssakhov, Mohammad Rahimi-Gorji, B. C. Prasannakumara, Impact of magnetic dipole on ferromagnetic hybrid nanofluid flow over a stretching cylinder, Phys. Scr. 96 (4) (2021), 045215, https://doi.org/10.1088/1402-4896/abe324.
[16] M. Irfan, M. Khan, W.A. Khan, Impact of non-uniform heat sink/source and convective condition in radiative heat transfer to Oldroyd-B nanofluid: a revised proposed relation, Phys. Lett. A 383 (4) (2019) 376–382, https://doi.org/10.1016/j.physleta.2018.10.040.
[17] M. Ramzan, N. Shaheen, S. Kadry, Y. Ratha, Y. Nam, Thermally stratified Darcy Forchheimer flow on a moving thin needle with homogeneous heterogeneous reactions and non-uniform heat source/sink, Appl. Sci. 10 (2) (2020), https://doi.org/10.3390/app10020432.
[18] M. Radhika, R.J.P. Gowda, R. Naveenkumar, Siddabasappa, B.C. Prasannakumara, Heat transfer in dusty fluid with suspended hybrid nanoparticles over a melting surface, Heat Transf (2020), https://doi.org/10.1002/htj.21972.
[19] A. Ali, S. Mumraiz, S. Nawaz, M. Awais, S. Asghar, Third-grade fluid flow of stretching cylinder with heat source/sink, J. Appl. Comput. Mech. 6 (2020) 1125–1132, https://doi.org/10.22055/jacm.2020.31275.1850.
[20] M. Faisal, I. Ahmad, T. Javed, Numerical simulation of mixed convective 3D flow of a chemically reactive nanofluid subject to convective Nield's conditions with a nonuniform heat source/sink, Heat Transf. 50 (1) (2021) 352–369, https://doi.org/10.1002/htj.21880.
[21] P.-.Y Xiong, Aamir Hamid, Yu-Ming Chu, M. Ijaz Khan, R.J. Punith Gowda, R. Naveen Kumar, B.C. Prasannakumara, Sumaira Qayyum, Dynamics of multiple solutions of Darcy–Forchheimer saturated flow of Cross nanofluid by a vertical thin needle point, Eur. Phys. J. Plus 136 (3) (2021) 315, https://doi.org/10.1140/epjp/s13360-021-01294-2.
[22] L.A. Lund, Z. Omar, J. Raza, I. Khan, Magnetohydrodynamic flow of Cu–Fe3O4/H2O hybrid nanofluid with effect of viscous dissipation: dual similarity solutions, J. Therm. Anal. Calorim. 143 (2) (2021) 915–927, https://doi.org/10.1007/s10973-020-09602-1.
[23] Z. Shah, E.O. Alzahrani, W. Alghamdi, M.Z. Ullah, Influences of electrical MHD and Hall current on squeezing nanofluid flow inside rotating porous plates with viscous and joule dissipation effects, J. Therm. Anal. Calorim 140 (3) (2020) 1215–1227, https://doi.org/10.1007/s10973-019-09176-7.
[24] K. Hong, R. Alizadeh, M.V. Ardalan, A. Nourbakhsh, N. Karimi, Y. Yang, Q. Xiong, Numerical study of nonlinear mixed convection inside stagnation-point flow over surface-reactive cylinder embedded in porous media, J. Therm. Anal. Calorim. 141 (2020) 1889–1903, https://doi.org/10.1007/s10973-019-09245-x.
[25] A.S. Idowu, M.T. Akolade, T.L. Oyekunle, J.U. Abubakar, Nonlinear convection flow of dissipative Casson nanofluid through an inclined annular microchannel with a porous medium, Heat Transf (2020), https://doi.org/10.1002/htj.22033.
[26] A.M. Rashad, S. Abbasbandy, Ali J. Chamkha, Non-Darcy natural convection from a vertical cylinder embedded in a thermally stratified and nanofluid-saturated porous media, J. Heat Transf. 136 (2014), 022503.
[27] S.M.M. El-Kabeir, A.J. Chamkha, A.M. Rashad, Effect of thermal radiation on non-darcy natural convection from a vertical cylinder embedded in a nanofluid porous media, J Porous Media 17 (2014) 269–278.
[28] M.A Mansour, Sadia Siddiqa, Rama Subba Reddy Gorla, A.M Rashad, Effects Of heat source and sink on entropy generation and MHD natural convection of Al2O3-Cu/water hybrid nanofluid filled with square porous cavity, Thermal Sci. Eng. Progress 6 (2018) 57–71.

[29] E.R. EL-Zahar, A.M. Rashad, W. Saad, L.F. Seddek, Magneto-hybrid nanofluids flow via mixed convection past a radiative circular cylinder, Sci Rep 10 (1) (2020) 10494.
[30] F. Bezdidi-Tehrani, M. Sedaghatnejad, S.I. Vasefi, Investigation of mixed convection and particle dispersion of nanofluids in a vertical duct, Proc IMechE Part C: J Mech. Eng. Sci. 230 (20) (2016) 3691–3705.
[31] S.I. Vasefi, F. Bazdidi-Tehrani, Mohammad Sedaghatnejad, A. Khabazipur, Optimization of turbulent convective heat transfer of CuO/Water nanofluid in a square duct:an artificial neural network analysis, J. Thermal Anal. Calorimetry 143 (2019) 2026–2040.
[32] S.I. Vasefi, F. Bazdidi-Tehrani, L. Reyhani, Assessment of mean and fluctuating velocity and temperature of CuO/Water Nanofluid in aHorizontal Channel: large Eddy Simulation, Numerical Heat Transfer, Part A: Appl.. 74 (2018) 1520–1538.
[33] F. Bazdidi-Tehrani, A. Khabazipur, S.I. Vasefi, Flow and heat transfer analysis of TiO2/water nanofluid in a ribbed flat-plate solarcollector, Renew. Energy 122 (2018) 406–418.
[34] F. Bazdidi-Tehrani, S.I. Vasefi, A. Khabazipur, Scale-adaptive simulation of turbulent mixed convection of nanofluids in a vertical duct, J.Thermal Anal. Calorimetry 131 (2018) 3011–3023.
[35] F. Bazdidi-Tehrani, S.M.K. Mohamadi, S.I. Vasefi, Evaluation of turbulent forced convection of non-Newtonian aqueous solution of CMC/CuOnanofluid in a tube with twisted tape inserts, Adv. Powder Technol. 31 (2020) 1100–1113.
[36] Y. Lin, L. Zheng, Marangoni boundary layer flow and heat transfer of copper-water nanofluid over a porous medium disk, AIP Adv. 5 (2015), 107225.